JOURNAL OF MATERIALS SCIENCE 27 (1992) 3726–3732

Similarities in the low-energy configurations of dislocations and vortices

M. J. MARCINKOWSKI
Department of Mechanical Engineering, University of Maryland, College Park, MD 20742, USA

It is shown that vortices and dislocations can be treated as virtually identical from both a physical and mathematical perspective. This allows the lowest-energy configurations of such defects to be predicted. In particular, it is suggested that, similar to the way in which a dislocation cell structure forms at high deformations, an analogous vortex cell structure is generated at high fluid velocities. In addition, both arrangements are believed to underlie the concept of turbulence.

1. Introduction

An extraordinarily close relationship has been shown to exist between the deformation of solids and the flow of fluids [1, 2]. Some of these similarities that are relevant to the present study are listed in Table I. More generally, elastic deformation may be likened to irrotational flow, while plastic deformation can be equated to rotational flow. Whereas dislocations underlie the basis of plasticity, vortices represent the fundamental unit of rotational flow. Dislocations and vortices fall under the category of line defects and have a common mathematical and physical basis. This commonality will be exploited in the present study to predict the most likely arrangements of these defects for various deformations and flows.

2. Individual dislocations and vortices

The radial lines in Fig. 1a correspond to equipotentials associated with an isolated vortex, whereas the circles represent the direction of flow induced by these potentials [3, 4]. When a uniform momentum field, P, given by

$$P_i = \rho v_i \tag{1}$$

is superimposed on the isolated vortex field, the configuration in Fig. 1b obtains. The quantity v_i in Equation 1 denotes the velocity vector, whereas ρ denotes the fluid density, which will be assumed to be constant (i.e. incompressible flow). The astonishing feature of Fig. 1b is its close resemblance to that of an edge-type dislocation. In the present case, however, the crystallographic planes are replaced by equipotential lines. The flow is at right angles to these lines from left to right. How could this important similarity have been overlooked for so long? One possible reason is the habit of including only the streamlines in the construction of most flow patterns [3, 4].

The vortex in Fig. 1b has induced extra equipotential lines into the momentum field, similar to the way in which the edge dislocation in Fig. 2a has introduced an extra half-plane into the originally perfect crystal lattice. The similarity is made more striking by redrawing Fig. 1b as shown in Fig. 2b, wherein the streamlines have been omitted.

Suppose now that a clockwise Burgers circuit is taken about the quantized lattice dislocation (solid symbol) in Fig. 2a, as shown by the arrows. The closure failure of this circuit is denoted by the dotted arrow and is precisely the Burgers vector, b, of the enclosed dislocation. More precisely, it may be written as [1]

$$b_i = \Delta u_i = \oint \mathrm{d}u_i = \oint \partial_j u_i \mathrm{d}x_j = \oint \beta_{ji} \mathrm{d}x_j \tag{2}$$

where β_{ji} is the distortion given by

$$\beta_{ji} = \partial_j u_i \tag{3}$$

while u_i is the plastic displacement. In particular, Δu_i represents the total plastic displacement associated with the dislocation, which is equivalent to the width of the extra half-plane in Fig. 2a. When the body containing the dislocation is taken to be finite, as is the case in Fig. 2a, then it is necessary that an array of surface dislocations (dotted symbols) be distributed upon it in order to satisfy the stress-free boundary conditions [5]. Unlike the lattice dislocation, the surface dislocations are of infinitesmal strength and continuously distributed, reflecting the resultant change in the surface profile. Furthermore, the law of the conservation of Burgers vectors must be obeyed; namely [6]

$$b_L + b_S = 0 \tag{4}$$

which states that the sum of the Burgers vectors of the lattice dislocation and its corresponding surface dislocations must add up to zero. Conversely, the sum of all the surface dislocations must be equal in strength but opposite in sign to that of the lattice dislocation.

Similar to the case of a dislocation, a clockwise Burgers circuit may be drawn about the quantized

0022–2461

TABLE I Correspondence between fluid flow and deformation of solids

Fluids	Solids
Irrotational flow	Elastic deformation
Rotational flow	Plastic deformation
Vortices	Dislocations
Momentum, P_i	Stress, σ_{ij}
Potential, ϕ	Displacement, u_i
Velocity, v_i	Distortion, β_{ij}
Circulation, Γ	Burgers vector, b_i
Vorticity, w_i	Dislocation density, α_{ij}
Density, ρ	Elastic constant, G
Kinetic energy	Strain energy
Conservation law for circulation	Conservation law for Burgers vector
Vortex boundary	Grain boundary
Vortex boundary energy, E_{VB}	Grain boundary energy, E_{DB}
Flow-free boundary conditions	Traction-free boundary considerations
Irrotational flow along curved channel	Elastic bending
Rotational flow along curved channel	Plastic bending
Retarded flow	Tension
Enhanced flow	Compression
Fluid turbulence associated with formation of vortex cells	Solid turbulence associated with formation of dislocation cells

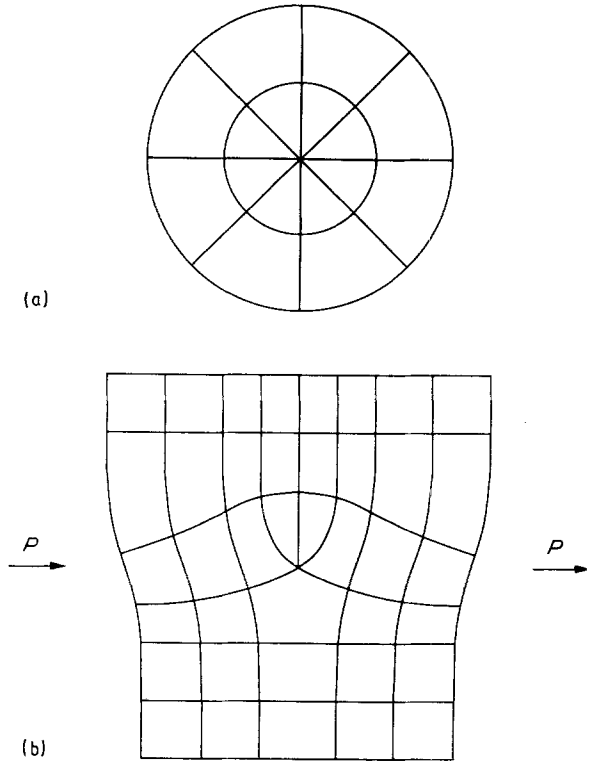

Figure 1 Vortex in the (a) absence, (b) presence of an applied momentum field, P.

vortex (solid symbol) in Fig. 2b. The closure failure is depicted by the dotted arrow and corresponds to the circulation, Γ, of the enclosed vortex. Mathematically, it can be expressed as [1]

$$\Gamma = \Delta\phi = \oint d\phi = \oint \partial_i \phi dx_i = \oint v_i dx_i \quad (5)$$

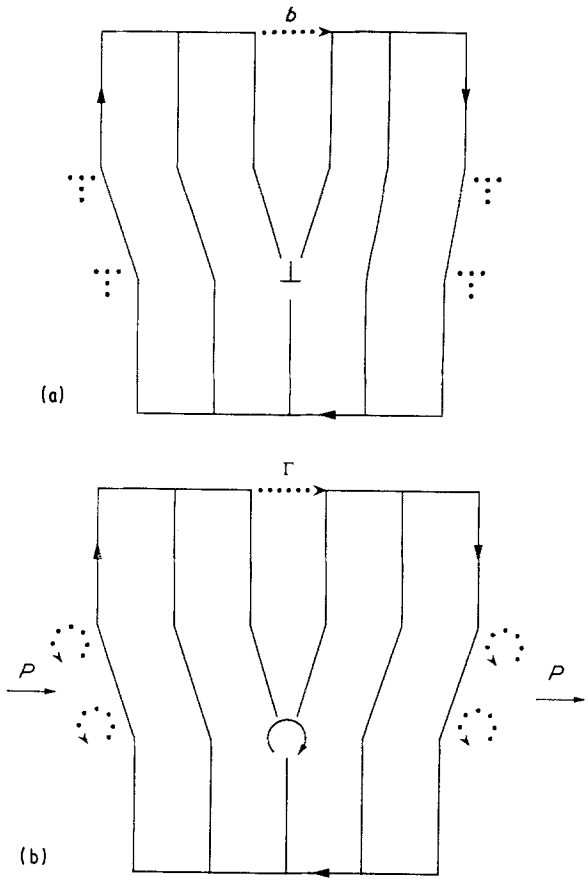

Figure 2 Similarity between (a) dislocation and (b) vortex.

where

$$v_i = \partial_i \phi \quad (6)$$

The quantity $\Delta\phi$ is simply the number of extra potential lines about the Burgers circuit. Unlike b_i, which is a vector, Γ is a scalar. The striking correspondences between the various quantities in Equations 2 and 5 can be seen more clearly by reference to Table I. When the fluid body in Fig. 2b is taken as finite, it is required that its surfaces be covered with a certain distribution of surface vortices (dotted symbols), similar to the case for a dislocation. Likewise, the following conservation law for circulation must hold [1]:

$$\Gamma_L + \Gamma_S = 0 \quad (7)$$

where Γ_L is the circulation of the quantized vortex, whereas Γ_S includes that from all of the continuously distributed surface vortices.

3. The close analogy between tilt-type boundaries in liquids and solids

As the lattice dislocation in Fig. 2a moves toward the rightmost surface, it attracts the surface dislocations toward it, as illustrated in Fig. 3a. Once surface contact is achieved, the quantized lattice dislocation begins to annihilate some of the surface dislocations, in turn forming a small step, as can be observed in Fig. 3b. Finally, when annihilation is complete, a surface step of length b, the Burgers vector of the quantized dislocation, is created. This can be seen by reference to Fig. 3c.

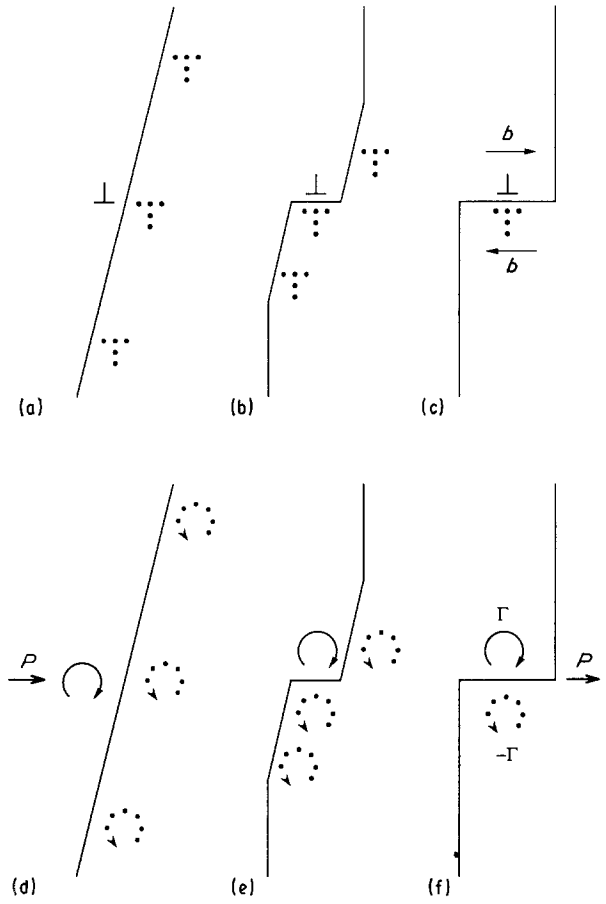

Figure 3 Sequence of events in the annihilation of (a–c) a quantized dislocation and (d–f) a vortex, as it meets a free surface.

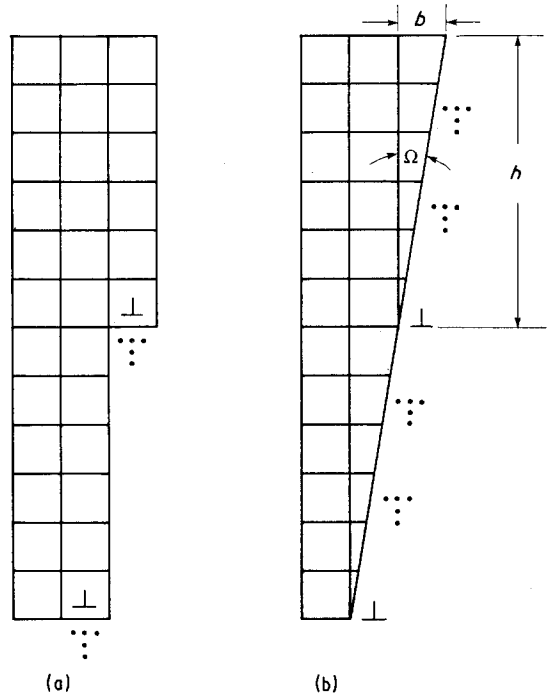

Figure 4 Dislocation configuration in (b) obtained after stepped surface in (a) is flattened by elastic displacements.

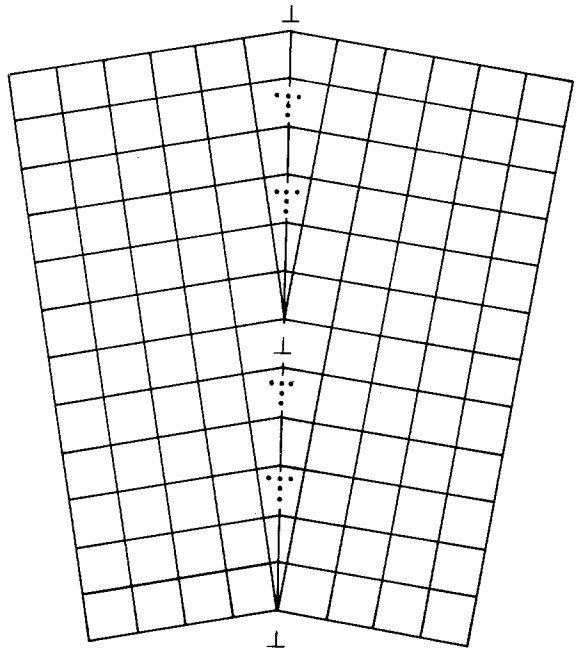

Figure 5 Dislocation tilt boundary within a solid.

In a similar manner, as the quantized vortex in Fig. 2b nears the rightmost surface, it attracts surface vortices to it in the manner of Fig. 3d. As a result, the potential line profile is distorted in the vicinity of the vortices. On contacting the surface, the quantized vortex begins to annihilate the surface vortices, in turn creating a small step in the equipotential line, as shown in Fig. 3e. Complete annihilation can be seen in Fig. 3f where the circulation associated with the quantized vortex just cancels those of all the surface vortices. As a result, a step of width Γ is formed in an otherwise uniform equipotential pattern.

Consider next the uniform array of ledges in Fig. 4a of the type already discussed in connection with Fig. 3c. If the ledges are next elastically flattened to produce a planar surface, the configuration shown in Fig. 4b obtains. The surface is seen to consist of an array of localized lattice dislocations connected by a continuous array of surface dislocations, all obeying Equation 4. When the configuration in Fig. 4b is joined to its mirror image, the symmetric tilt-type grain boundary of Fig. 5 obtains. This model has been argued to be the correct alternative [7, 8] to the classical one first proposed by Burgers [9]. The grains, or cells, adjoining the grain boundary are rotated by an angle, 2Ω, relative to one another. From the geometry of Fig. 4b and Fig. 5, this angle can be written as

$$2\Omega = 2 \tan^{-1}\left(\frac{b}{h}\right) \tag{8}$$

where h is the spacing between lattice dislocations. For small misorientations, this reduces to [10]

$$\Omega \simeq \frac{b}{h} \tag{9}$$

The vortex counterpart of the stepped surface in Fig. 4a is shown in Fig. 6a and consists of a uniform array of ledges in potential space of the type illustrated in Fig. 3f. When this vortex configuration is rearranged along the lines used to generate the dislocation array in Fig. 4b, the arrangement shown in Fig. 6b is the result. In a similar fashion, it is seen to

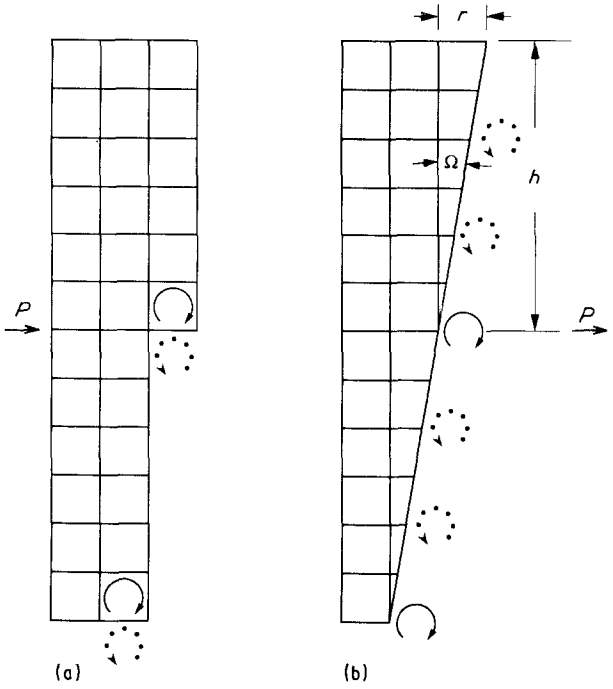

Figure 6 Fluid counterparts of the dislocated solids in Fig. 4.

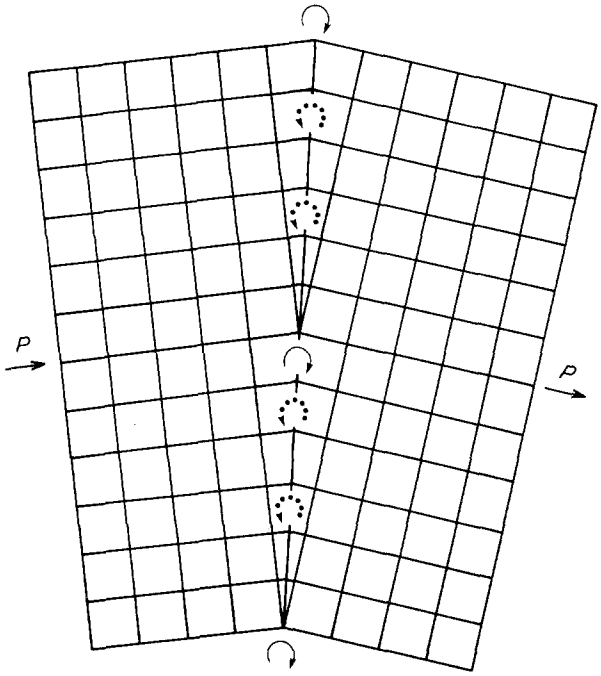

Figure 7 Vortex tilt boundary within a liquid.

consist of a uniform array of quantized vortices connected by a continuous distribution of surface vortices. It is clear from this configuration that the velocity profile across the rightmost surface is no longer uniform, as was the case in Fig. 6a.

When a cell of the type given by Fig. 6b is joined to its mirror image, the configuration shown in Fig. 7 is obtained. It can be seen from this drawing that the velocity is uniform everywhere except in the vicinity of the boundary, where a sharp change in direction and velocity occurs. From the geometry of Fig. 6b and Fig. 7, the change in direction of flow across the vortex boundary may be written as

$$2\Omega = 2 \tan^{-1}\left(\frac{r}{h}\right) \tag{10}$$

where r is the step length associated with a quantized vortex, which can be related to its circulation by [1]

$$r = \frac{\Gamma}{v} \tag{11}$$

where v is the fluid velocity at the step. Combining Equations 10 and 11 yields

$$2\Omega = 2 \tan^{-1}\left(\frac{\Gamma}{vh}\right) \tag{12}$$

which is the fluid analogue of Equation 8 for dislocations. For small angles, Equation 12 becomes

$$\Omega \simeq \frac{\Gamma}{vh} \tag{13}$$

From Equation 11, it follows that the velocity at the step must be chosen to match that of the uniform velocity stream within the cells. Under this condition, fluid will be directed uniformly from one cell to the other.

The mathematical conditions that must be satisfied in order for the surface in Fig. 3a to be traction-free is as follows:

$$\sigma_{ij} n_j = 0 \tag{14}$$

where σ_{ij} is the stress field within the solid, while n_j is the normal to the surface. In a similar manner, the condition that the velocity component normal to the liquid surface in Fig. 3d vanish is given by

$$P_i n_i = 0 \tag{15}$$

Clearly, Equations 14 and 15 are not satisfied in Figs 4b and 6b, respectively, which in turn allows tractions and flow to be transmitted across the boundaries in Figs 5 and 7, respectively. On the other hand, the conservation laws for Burgers vectors and circulations embodied in Equations 4 and 7, respectively, must always be obeyed.

The boundary in Fig. 5 is essentially dipolar in nature so that the dislocations screen one another's stress fields. The screening distance is of the order of the dislocation spacing or $h/2$. The energy per unit length of the boundary can thus be written in terms of the self-energy of a single dislocation wherein the screening distance is used for the cut-off distance, giving [1]

$$E_{DB} = \frac{Gb^2}{2\pi h} \ln\left(\frac{h}{2r_o}\right) \tag{16}$$

In the case of fluids, the velocity fields associated with the vortex wall in Fig. 7 are screened due to their dipole nature. As for dislocations, the energy per unit length of such walls can be written in terms of the self-energy of an individual vortex as follows:

$$E_{VB} = \frac{\pi\Gamma^2}{4\pi} \ln\left(\frac{h}{2r_o}\right) \tag{17}$$

where, once again, $h/2$ is used for the cut-off length [1]. The similarity of this relation with Equation 16 is obvious.

4. Comparison between bending and flow along a curved channel

It has been shown [11] that the elastic bending of a beam can be described in terms of a unique distribution of surface dislocations, as illustrated in Fig. 8a. The displacement of the nearly vertical lattice planes show that the fibres above the neutral axis are in tension, while those below are under compression.

As can be seen in Fig. 8b, the case of irrotational fluid flow along a curved channel can be represented in terms of a distinct array of surface vortices and is remarkably similar to that for the bent beam. In this case, the array of vortices on the topmost surface retards the flow from the external field P. Those on the bottommost surface, however, enhance the flow rate. This is clear from the spacing of the nearly vertical equipotential lines, which now take the place of lattice planes in the bent beam. Carrying the analogy still further, an increased flow rate corresponds to compression, while retarded flow corresponds to tension. The surface dislocations and vortices in Figs 8a and b, respectively, are seen to obey the conservation laws of Equations 4 and 7, respectively.

As the bending in Fig. 8a is increased, the stresses within the beam become sufficiently high to generate and propagate lattice dislocations. These are shown in Fig. 9a and are seen to consist of a continuous distribution of tilt boundaries [11] of the type already discussed in connection with Fig. 5. It is this arrangement that leads to the greatest reduction in elastic strain energy within the beam.

In a similar manner, as the momentum field along the curved channel is increased, vortex nucleation and multiplication within the fluid is enhanced, leading to the rotational flow shown in Fig. 9b. It is seen to consist of a continuous distribution of vortex walls of the type illustrated in Fig. 7. This arrangement is quite stable and leads to a significant reduction in the kinetic energy of the fluid.

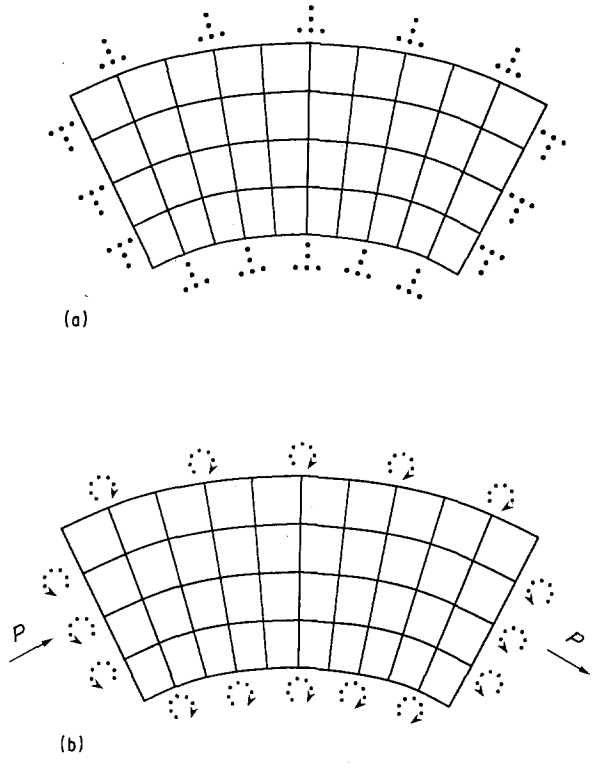

Figure 8 (a) Elastic bending of a beam, (b) irrotational flow along a curved channel.

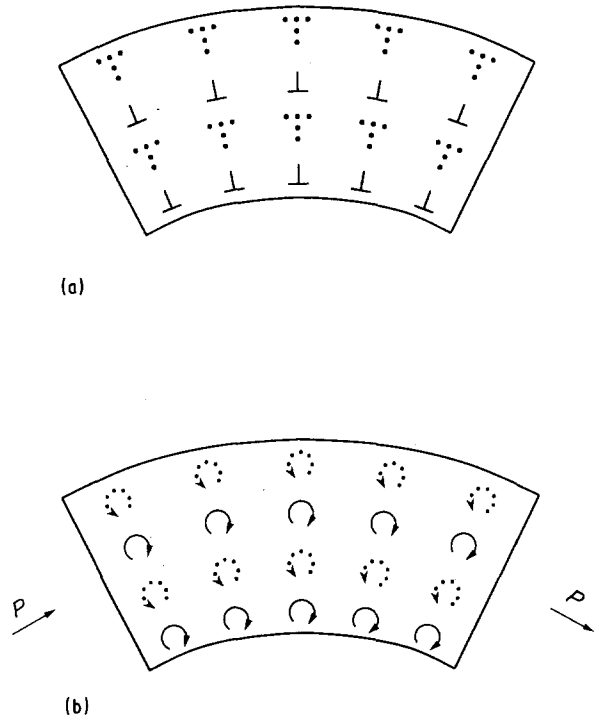

Figure 9 (a) Plastic bending of a beam, (b) rotational flow along a curved channel.

5. Correspondence between large deformations and high-velocity flows

As early as 1913, Darwin [12, 13] concluded from his X-ray studies that crystals were subdivided into mosaic blocks. Later electron microscopy studies showed that these blocks were in fact cells delineated by dislocation walls [14]. A model for these walls was subsequently developed in terms of classical grain boundaries [15] and later modified to include surface dislocations [16]. The final result is shown in Fig. 10a. Such a structure develops with increasing degrees of plastic deformation. It is seen to consist of boundaries of the type discussed earlier in connection with Fig. 5. The solid lines correspond to slip planes over which the lattice dislocations have passed on their way to the cell walls. Because of space limitations, the surface dislocations within the boundaries are indicated by a single dot. It is the dipole nature of such walls that give them the lowest energy of any possible dislocation arrangement, in accordance with Equation 16.

As in the case of dislocations, the vortices are not expected to be arranged randomly but rather take the form illustrated in Fig. 10b. Again, the solid-line segments represent the planes over which the quantized vortex lines have moved on their way to the cell walls. The vortex walls are of the type previously discussed in connection with Fig. 7. Because of space limitations, the surface vortices in Fig. 10b are denoted by single dots. Here again, it is the dipole nature of such walls

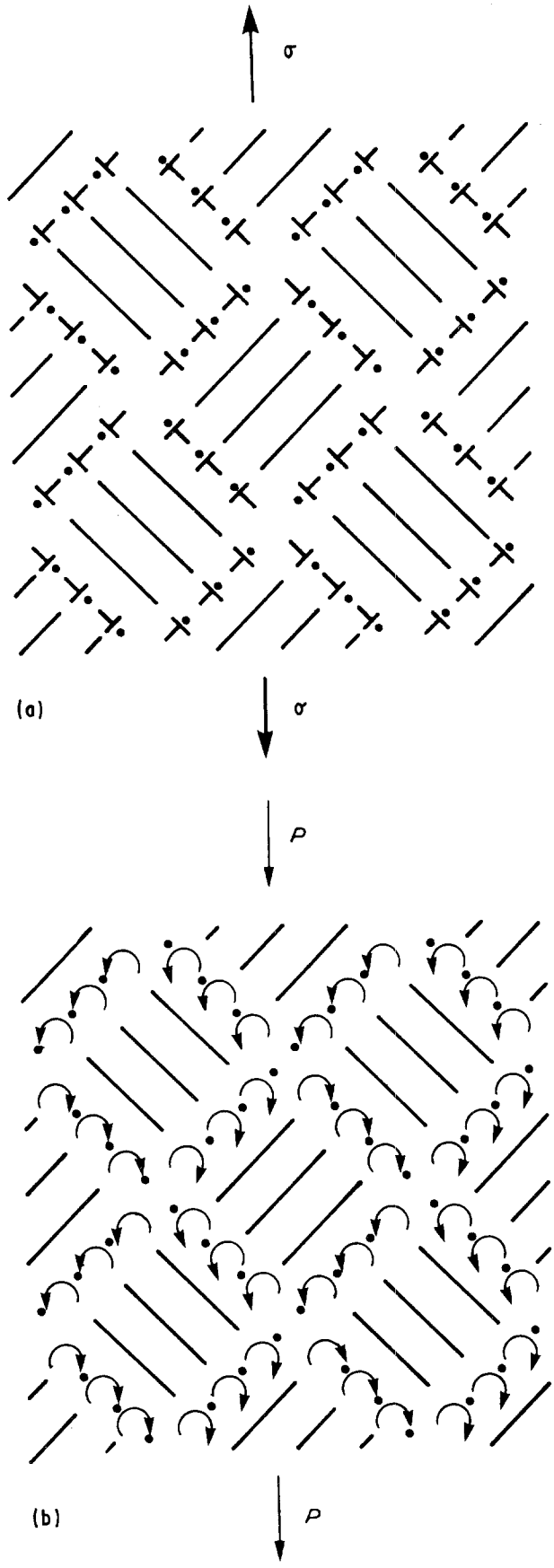

Figure 10 Generation of (a) dislocation, (b) vortex cell structure within a solid and liquid, respectively, in response to the applied stress and momentum fields, respectively.

that gives them their low energy, in accordance with Equation 17.

Perhaps the single most distinguishing feature of Fig. 10a is that an originally perfectly periodic arrangement of crystalline planes has been broken up into a chaotic jumble of misaligned cells at sufficiently high plastic strains. For flow to continue, both the slip plane and direction must change discontinuously from one cell to its neighbour. This type of deformation may be labelled as turbulent, in contrast to the more laminar flow that occurs on a single slip system within a perfect crystal.

Similarly, the characteristic aspect of Fig. 10b is the break-up of an originally "crystallographic" alignment of equipotential lines into a chaotic maze of misoriented cells after the attainment of some critical velocity or Reynolds number [17]. The direction of flow is forced to change repeatedly from one cell to another, similar to that which was encountered in solids, and thus may be termed turbulent. At low velocities the flow takes place along a single direction and is designated as laminar.

6. Summary and conclusions

Once it is realized that uniform fluid flow can be represented in terms of equally spaced planes of constant potential, much like those that comprise a crystal lattice, the connection between vortices and dislocations is immediate. In particular, the superposition of a vortex on to this uniform flow gives rise to extra equipotential half-planes analogous to the extra half-planes associated with an edge-type dislocation within a crystal. Upon recognition of this correspondence, the physics and mathematics for both types of line defect are seen to be identical. It then becomes possible to formulate models of the most likely arrangements of such defects, based on lowest-energy considerations. More specifically, it is suggested that similar to the way in which dislocations align themselves into cell walls at large deformations, vortices do the same at high flow rates. It is concluded therefrom that such arrangements form the common basis of turbulence in both liquids and solids.

References

1. M. J. MARCINKOWSKI, *Phys. Status Solidi (b)* **152** (1989) 9.
2. *Idem, Phil. Mag.* **A 62** (1990) 363.
3. L. M. MILNE-THOMSON, "Theoretical Hydrodynamics" (MacMillan, London, 1938) p. 178.
4. N. E. KOCHIN, I. A. KIBEL and N. V. ROZE, "Theoretical Hydrodynamics", translated from Russian by D. Boyanovitch, edited by J. R. M. Radok (International Publishers, New York, 1964) p. 258.
5. K. JAGANNADHAM and M. J. MARCINKOWSKI, *Phys. Status Solidi (a)* **50** (1978) 293.
6. M. J. MARCINKOWSKI and E. S. P. DAS, *Int. J. Fracture* **10** (1974) 181.
7. M. J. MARCINKOWSKI, *Phys. Status Solidi (a)* **96** (1986) 425.
8. *Idem, Phil. Mag. Lett.* **62** (1990) 19.
9. J. M. BURGERS, *Proc. Kon. Nederl. Akad. Wetensch.* **42** (1939) 293.
10. J. P. HIRTH and J. LOTHE, "Theory of Dislocations" (McGraw-Hill, New York, 1968) p. 645.
11. M. J. MARCINKOWSKI, *Phys. Status Solidi (b)* **126** (1984) 527.
12. C. G. DARWIN, *Phil. Mag.* **27** (1934) 315.
13. *Idem, ibid.* **27** (1934) 675.

14. J. D. EMBURY, A. S. KEH and R. M. FISHER, *Trans. Met. Soc. AIME* **236** (1966) 1252.
15. D. KUHLMANN-WILDORF and J. H. VAN DER MERWE, *Mater. Sci. Engng* **55** (1982) 79.
16. M. J. MARCINKOWSKI, *Phys. Status Solidi* (*a*) **94** (1986) 489.
17. K. OSWATITSCH, "Physikalische Grundlagen der Strömungslehre", in "Handbuch der Physik", edited by S. Flügge (Springer, Berlin, 1959) Vol. VIII/1.

Received 12 March
and accepted 1 July 1991